

**Short Contribution**

## Depth Distribution of the Subtropical Gyre in the North Pacific

TANGDONG QU\*

*International Pacific Research Center, SOEST, University of Hawaii, Honolulu, HI 96822, U.S.A.*

(Received 31 May 2001; in revised form 19 September 2001; accepted 20 September 2001)

**Large-scale aspects of the North Pacific subtropical gyre have been investigated using a climatology of temperature and salinity (World Ocean Atlas 1998). In the central and eastern parts of the basin, the axis of the subtropical gyre, defined as the meridional maximum of dynamic height, tends to move poleward from about 25°N near the surface to about 40°N in the upper intermediate layers. In the western part of the basin, the axis is seen at about 30°N, remaining almost unchanged with depth. Striking features associated with this vertical distribution include a northward shift of the bifurcation latitude of the North Equatorial Current at increasing depth and a barotropic nature of the confluence point between the Kuroshio and Oyashio at their respective western boundaries. The former occurs at about 14°N near the surface and extends north of 20°N at depths around 800 m. The latter, situated at about 36.4°N off Japan, does not appear to have a strong signature of depth-dependence. While some of these results are already known from sporadic hydrographic observations, they have not hitherto been represented in a three-dimensional climatology.**

Keywords:

- Bifurcation,
- confluence,
- depth distribution,
- subtropical gyre,
- North Pacific.

### 1. Introduction

A prominent feature of the subtropical gyre in the North Pacific is its poleward contraction on denser waters. Reid and Arthur (1975) provided the first picture to demonstrate this phenomenon. According to their results, the subtropical gyre recognized at the sea surface (Reid, 1961) tends to extend downward to depths as great as 2500 m, but is found to be progressively weaker and farther poleward with depth. This picture has been a benchmark for many theoretical, observational, and modeling studies of the North Pacific subtropical gyre (e.g., Rhines and Young, 1982; Luyten *et al.*, 1983; Huang, 1988). However, Reid and Arthur based their study on early hydrographic observations, and as a result of data limitation the three-dimensional structure of the North Pacific subtropical gyre was not carefully examined in their study. Until recent times a comprehensive description of the exact position of the North Pacific subtropical gyre, including its zonal distribution and depth dependence, was not available.

Interest in the depth distribution of the subtropical gyre has increased recently in response to the need to better understand the Subtropical Cell (STC, McCreary and Lu, 1994) which allows exchange between the subtropical and equatorial oceans. In the North Pacific, the equatorward-flowing subsurface branch of the STC involves the North Equatorial Current (NEC) and the Mindanao Current (Lukas *et al.*, 1991). Recent study suggests that the Luzon Undercurrent (LUC, Qu *et al.*, 1997) also participates in this circulation. The presence of the LUC is known to be related to the depth dependence of the Mindanao Dom (Masumoto and Yamagata, 1991; Qu *et al.*, 1999), but its connection with the basin-scale circulation of the North Pacific needs to be investigated further.

This study seeks a better description of the subtropical gyre in the North Pacific: its zonal distribution and depth dependence, using the climatological data recently released by NOAA/NESDIS/NODC (World Ocean Atlas 1998) in the region 10°N–50°N and 120°E–80°W. Special attention is paid to the bifurcation of the NEC and the confluence of the Kuroshio/Oyashio near western boundary.

\* E-mail address: tangdong@soest.hawaii.edu

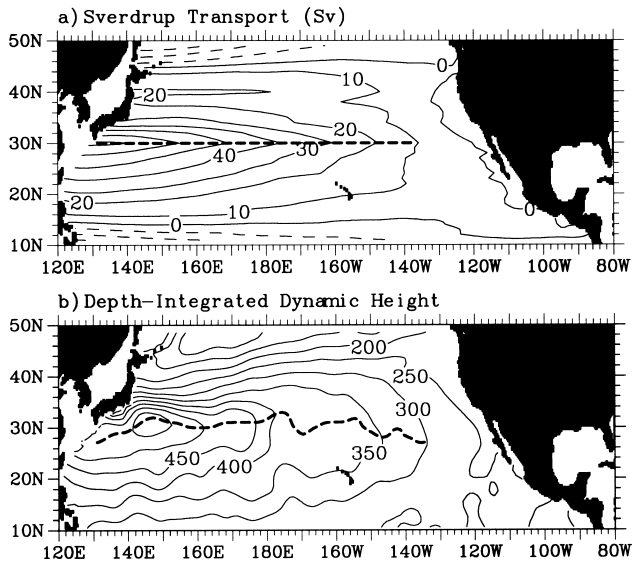


Fig. 1. (a) Sverdrup transport in Sv ( $1 \text{ Sv} = 10^6 \text{ m}^3\text{s}^{-1}$ ) calculated from Hellerman-Rosenstein (1983) wind stress, and (b) depth integrated dynamic height relative to 2000 db in  $\text{m}^2$  calculated from the climatology of temperature and salinity (World Ocean Atlas 1998). The value of  $1200 \text{ m}^2$  has been subtracted before plotting in (b). The heavy dashed lines indicate the east-west axis of the subtropical gyre.

## 2. Vertically Integrated Circulation

Sverdrup transport calculated from Hellerman and Rosenstein's (1983) annual mean wind stress provides a basic picture of the vertically integrated circulation in the North Pacific (Fig. 1(a)). In this picture, the east-west axis of the subtropical gyre is seen along  $30^\circ\text{N}$ . Two zero-transport lines, located at about  $15^\circ\text{N}$  in the south and about  $45^\circ\text{N}$  in the north, form the boundaries between the subtropical and tropical gyres and between the subtropical and subpolar gyres, respectively.

Depth-integrated dynamic height relative to 2000 db (Fig. 1(b)) shows essentially the same pattern as Sverdrup transport (Fig. 1(a)) in the interior ocean. Despite several small-scale phenomena, the east-west axis of the subtropical gyre, defined as the meridional maximum of dynamic height, corresponds reasonably well with that derived from Sverdrup transport. The largest discrepancies are seen near the coast of Japan, where the Kuroshio and Oyashio come together about  $8^\circ$  farther south than that required by Sverdrup constraint (Fig. 1(a)), presumably as a result of bottom topography and nonlinear effect (Hurlburt *et al.*, 1996).

## 3. Depth Distribution

The poleward shift of the subtropical gyre with depth is markedly evident in maps of dynamic height (Figs.

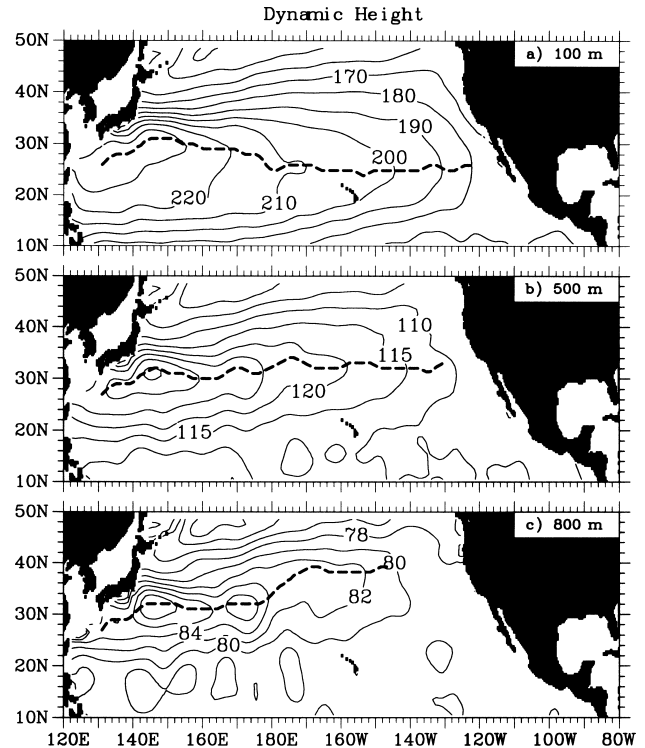


Fig. 2. Dynamic height relative to 2000 db in dyn-cm at (a) 100 m, (b) 500 m, and (c) 800 m depth. The heavy dashed lines indicate the axis of the subtropical gyre.

2(a)–(c)), with its greatest strength and broadest coverage at the sea surface. It moves entirely north of  $20^\circ\text{N}$  at depths around 800 m, leaving a broad region to the south dominated by a weak eastward flow. This weak eastward flow is also seen in Reid and Arthur's (1975) 1000/2000-db map and is consistent with the water mass distributions in the tropical western Pacific (Reid and Mantyla, 1978; Qu *et al.*, 1999). In the higher latitudes, the deep extension of the Kuroshio bifurcates at about  $175^\circ\text{E}$ , probably related to the bottom topography (Roden *et al.*, 1982; Mizuno and White, 1983). Its northern branch turns northeastward along the Emperor Sea Mounts and becomes almost unrecognizable east of  $180^\circ$ ; its southern branch turns southwestward and is dominated by eddy features associated with the recirculation west of  $180^\circ$  (Qiu, 1995).

Since water parcels are expected to flow along density surfaces, it is useful to look at the acceleration potential on isopycnals. Three isopycnals chosen are  $\sigma_\theta = 25.6, 26.8,$  and  $27.2$ , lying at depths 0–300 m, 400–700 m, and 700–1000 m, respectively. Maps of acceleration potential on isopycnal surfaces (Figs. 3(a)–(c)) resemble those of dynamic height at depths (Figs. 2(a)–(c)) in most details. In addition to those discussed above, the subtropical gyre is also seen to retreat westward on denser sur-

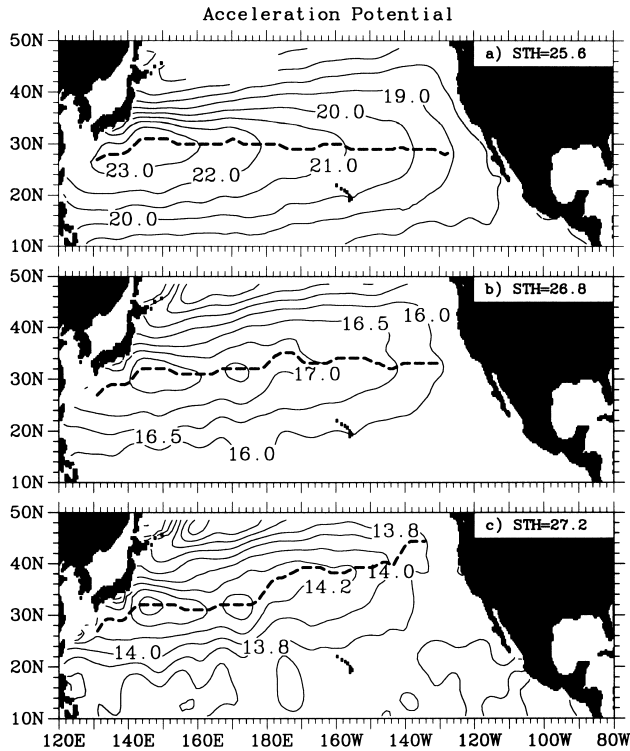


Fig. 3. Same as Fig. 2 except for acceleration potential in  $\text{m}^2\text{s}^{-2}$  on (a)  $25.6\sigma_\theta$ , (b)  $26.8\sigma_\theta$ , and (c)  $27.2\sigma_\theta$  surface.

faces, reflecting the westward intensification of wind-driven circulation.

### 3.1 East-west axis

The locations of the axis of the subtropical gyre (defined in Section 2) on different pressure and isopycnal surfaces are illustrated in Fig. 4. As already noted above, results derived from Sverdrup transport and depth-integrated dynamic height are generally identical, both showing an east-west axis of the subtropical gyre at about  $30^\circ\text{N}$ . In the central and eastern parts of the basin, roughly east of  $180^\circ\text{E}$ , the axis is seen to shift northward from about  $25^\circ\text{N}$  at 100 m to about  $38^\circ\text{N}$  at 800 m depth (Fig. 4(a)); but, in the west, it is basically east-west orientated and does not change significantly with depth. This vertical distribution is also evident along isopycnal surfaces (Fig. 4(b)).

On close inspection, the axis of the subtropical gyre is seen somewhat farther northward on  $25.6\sigma_\theta$  surface than at 100 m depth, presumably due to the fact that the depth of the  $25.6\sigma_\theta$  surface extends below 300 m in the central subtropical gyre. In the deeper layers, the circulation in the eastern portion of the gyre is more pronounced, and its axis appears to extend farther northeastward than that shown at 800 m. Given that the depth of  $27.2\sigma_\theta$  surface is only about 700 m near the eastern boundary (not shown),

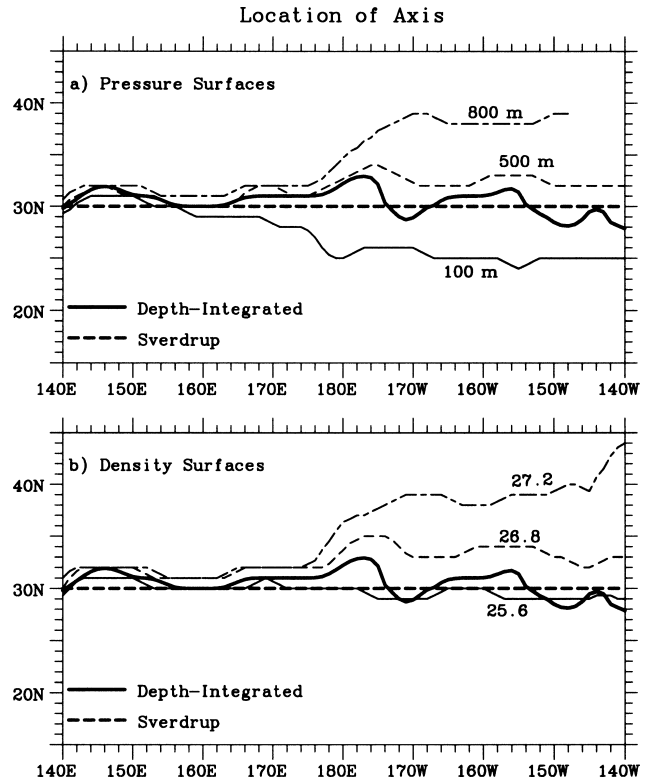


Fig. 4. Location of axis of the subtropical gyre on (a) pressure and (b) isopycnal surfaces.

this discrepancy reflects the shallower wind-driven circulation in the eastern portion of the subtropical gyre.

The axis of the subtropical gyre remains almost unchanged with depth in the western North Pacific (west of  $180^\circ\text{E}$ ). In addition to bottom topography and nonlinear effects (Hurlburt *et al.*, 1996), coastline orientation of the Kuroshio and its eastward extension is likely to be an important factor controlling the vertical distribution of the subtropical gyre in the western North Pacific.

### 3.2 Bifurcation of the NEC

An important implication of the results described above is that the bifurcation of the NEC moves northward as we progress to the deeper levels (Qu *et al.*, 1999). Given that the smoothed climatological data may not adequately resolve the narrow western boundary currents, we define the bifurcation of the NEC to be where the meridional transport within the  $5^\circ$ -longitude band from the coast is zero. At the sea surface, the bifurcation of the NEC occurs at about  $14^\circ\text{N}$  (Fig. 5(a)), in good agreement with earlier estimates both from synoptic observations and numerical simulations (Toole *et al.*, 1990; Qiu and Lukas, 1996). This bifurcation shifts northward at increasing depth, approaching nearly  $23^\circ\text{N}$  at 800 m. A significant manifestation of this northward shift of the NEC bifurca-

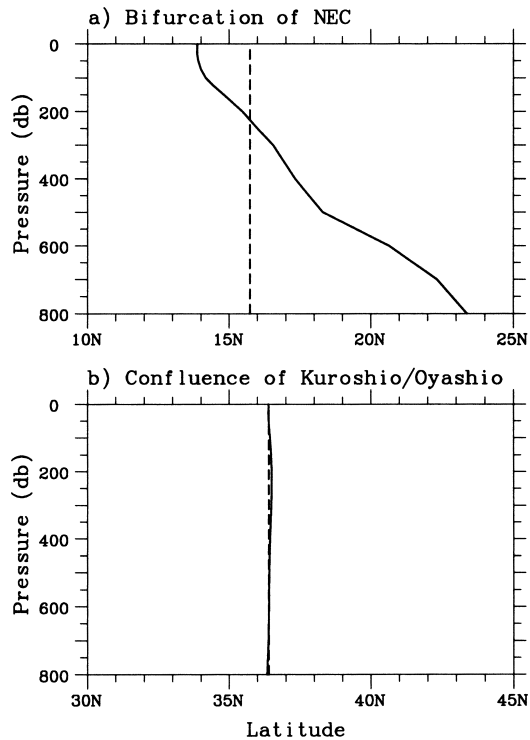


Fig. 5. Depth distribution of (a) bifurcation of the North Equatorial Current and (b) confluence of the Kuroshio/Oyashio. Dashed lines indicate the values calculated from depth-integrated dynamic height.

tion latitude with depth is the appearance of the LUC which flows southward as a subsurface countercurrent underlying the Kuroshio (Fig. 2), indicative of a component of the basin-scale circulation associated with the subtropical gyre.

### 3.3 Confluence of the Kuroshio/Oyashio

The confluence of the Kuroshio/Oyashio, defined in the same way as was stated for the bifurcation of the NEC, shows little depth dependence, remaining around  $36.4^{\circ}\text{N}$  at all depths from the surface down to 800 m (Fig. 5(b)). It has been reported in the literature that both the Kuroshio and Oyashio have a significant barotropic component at the western boundary (e.g., Kawai, 1972; Qu *et al.*, 2001). Here, we note that this barotropic signature is also markedly evident in their confluence point.

## 4. Summary

In this paper we have reported some preliminary results on the depth distribution of the North Pacific subtropical gyre. Although the climatological data used may not be especially appropriate for showing the detailed phenomena at the western boundary, they provide at least a basic background for understanding the basin-scale

structure of the subtropical gyre. Comprehensive analyses of the western boundary currents are to be made in the future. We hope this short report will serve as a guideline for future analyses.

Several conclusions are drawn from the present analysis. Most striking are those related to the poleward contraction of the subtropical gyre on denser waters. The axis of the subtropical gyre, characterized as a meridional maximum of dynamic height, is found to move northward from about  $25^{\circ}\text{N}$  near the surface to about  $40^{\circ}\text{N}$  at depths around 800 m in the central and eastern parts of the basin. This axis does not change significantly with depth in the western portion of the gyre, giving additional evidence for the barotropic nature of the Kuroshio Extension, already reported in the literature (Kawai, 1972; Mizuno and White, 1983; Qu *et al.*, 2001).

The bifurcation of the NEC occurs at about  $14^{\circ}\text{N}$  near the surface, and extends north of  $20^{\circ}\text{N}$  in the upper intermediate layers. This forms a sharp contrast with the condition of the Kuroshio/Oyashio confluence, in which the barotropic component seems to be dominant. While some of these results are already known from sporadic hydrographic observations, they have not hitherto been represented in a three-dimensional climatology.

Finally, we note that dynamic height fields at greater depths (up to 1500 m) and acceleration potential on denser surfaces (up to  $27.5\sigma_{\theta}$  surface) were also calculated (not shown). They do not appear to differ in any significant ways from those at 800 m and on the  $27.2\sigma_{\theta}$  surface.

## Acknowledgements

This research was partly supported by the Frontier Research System for Global Change through its sponsorship of the International Pacific Research Center (IPRC) and by the National Science Foundation through grant OCE00-95906. The author is grateful to J. McCreary, T. Yamagata, H. Mitsudera and K. Hanawa for many useful discussions. Thanks are also extended to K. Takeuchi, D. Henderson, and two anonymous reviewers for useful comments on the earlier manuscript. School of Ocean and Earth Science and Technology contribution number 5853, and IPRC contribution number IPRC-108.

## References

- Hellerman, S. and M. Rosenstein (1983): Normal monthly wind stress over the world ocean with error estimates. *J. Phys. Oceanogr.*, **13**, 1093–1104.
- Huang, R. X. (1988): On boundary value problems of the ideal-fluid thermocline. *J. Phys. Oceanogr.*, **18**, 619–641.
- Hurlburt, H. E., A. J. Wallcraft, W. J. Schmitz, P. J. Hogan and E. J. Metzger (1996): Dynamics of the Kuroshio/Oyashio current system using eddy-resolving models of the North Pacific Ocean. *J. Geophys. Res.*, **101**, 941–976.
- Kawai, H. (1972): Hydrography of the Kuroshio Extension. p. 235–354. In *Kuroshio: Physical Aspects of the Japan Cur-*

- rent, ed. by H. Stommel and K. Yoshida, University of Washington Press.
- Lukas, R., E. Firing, P. Hacker, P. L. Richardson, C. A. Collins, R. Fine and R. Gammon (1991): Observations of the Mindanao Current during the Western Equatorial Pacific Ocean Circulation Study. *J. Geophys. Res.*, **96**, 7089–7104.
- Luyten, J. R., J. Pedlosky and H. Stommel (1983): The ventilation thermocline. *J. Phys. Oceanogr.*, **13**, 292–309.
- Masumoto, Y. and T. Yamagata (1991): Response of the western tropical Pacific to the Asian winter monsoon: The generation of the Mindanao Dome. *J. Phys. Oceanogr.*, **21**, 1386–1398.
- McCreary, J. P. and P. Lu (1994): Interaction between the subtropical and equatorial ocean circulations: The Subtropical Cell. *J. Phys. Oceanogr.*, **24**, 466–497.
- Mizuno, K. and W. B. White (1983): Annual and interannual variability in the Kuroshio current system. *J. Phys. Oceanogr.*, **13**, 1847–1867.
- Qiu, B. (1995): Variability and energetics of the Kuroshio Extension and its recirculation gyre from the first two-year TOPEX data. *J. Phys. Oceanogr.*, **25**, 1827–1842.
- Qiu, B. and R. Lukas (1996): Seasonal and interannual variability of the North Equatorial Current, the Mindanao Current and the Kuroshio along the Pacific western boundary. *J. Geophys. Res.*, **101**, 12315–12330.
- Qu, T., T. Kagimoto and T. Yamagata (1997): A subsurface countercurrent along the east coast of Luzon. *Deep-Sea Res. I*, **44**, 413–423.
- Qu, T., H. Mitsudera and T. Yamagata (1999): A climatology of the circulation and water mass distribution near the Philippine coast. *J. Phys. Oceanogr.*, **29**, 1488–1505.
- Qu, T., H. Mitsudera and B. Qiu (2001): A climatological view of the Kuroshio/Oyashio system east of Japan. *J. Phys. Oceanogr.*, **31**, 2575–2589.
- Reid, J. L. (1961): On the geostrophic flow at the surface of the Pacific Ocean with respect to the 1000-decibar surface. *Tellus*, **13**, 489–502.
- Reid, J. L. and R. S. Arthur (1975): Interpretation of maps of geopotential anomaly for deep Pacific Ocean. *J. Mar. Res.*, **33** (Suppl.), 37–52.
- Reid, J. L. and A. W. Mantyla (1978): On the mid-depth circulation of the North Pacific Ocean. *J. Phys. Oceanogr.*, **8**, 946–951.
- Rhines, P. B. and W. R. Young (1982): A theory of the wind-driven circulation, I: Mid-ocean gyre. *J. Mar. Res.*, **40** (Suppl.), 559–596.
- Roden, G. I., B. A. Taft and C. C. Ebbesmeyer (1982): Oceanographic aspects of the Emperor Seamounts region. *J. Geophys. Res.*, **87**, 9537–9552.
- Toole, J., C. Millard, Z. Wang and S. Pu (1990): Observations of the Pacific North Equatorial Current bifurcation at the Philippine coast. *J. Phys. Oceanogr.*, **20**, 307–318.